TROPOSPHERIC HEAT SOURCES AND SINKS AT WASHINGTON, D.C., SUMMER 1961, RELATED TO THE PHYSICAL FEATURES AND ENERGY BUDGET OF THE CIRCULATION

PHILIP F. CLAPP and FRANCIS J. WINNINGHOFF

Extended Forecast Branch, U.S. Weather Bureau, Washington, D.C.

[Manuscript received February 8, 1963; revised June 11, 1963]

ABSTRACT

Estimates of atmospheric heating in the troposphere at Washington, D.C., for each successive 12 hr. during June and July 1961, were used to study the relation between local heating and the large-scale features of the circulation, to determine the local production of available potential energy, and to assist in interpreting cloud and radiation data from meteorological satellites.

Some interesting inter-connections are found between heating and the circulation: e.g., it is shown that there is a very critical phase relation between heating and the temperature field which is important in determining the generation or destruction of the atmosphere's potential energy. This suggests that special care is needed in designing numerical computations of diabatic heating.

A major effort should be directed to interpreting satellite data in terms of the atmospheric heat budget, because such global estimates may be useful (using a procedure suggested in this paper) in determining the world-wide distribution of regions of maintenance or destruction of potential energy.

1. INTRODUCTION

The importance of energy sources and sinks in determining the short- and long-period evolution of the general circulation has led to increasing attention to this subject. As an example from the extended-range point of view, Namias [14] has stressed the mutual interdependence between the thermal condition of the earth's surface and the atmospheric heat sources. This "feedback" acts in such a way that over long periods of time large-scale anomalies of the general circulation set up surface conditions (abnormal snow cover or ocean temperatures) which in turn influence the atmosphere's internal heat sources and sinks so as to perpetuate and perhaps amplify the original circulation anomalies. To qualitatively evaluate this influence, monthly charts of snow cover, ocean temperature anomalies, and soil moisture are being constructed for the Northern Hemisphere (Dickson [4]). One of the objectives of the work reported on here is to obtain quantitative estimates of these heat sources and to show how they are related to the structure and evolution of the circulation.

There are three methods of estimating atmospheric heating and cooling: by direct- or indirect-reading instruments (e.g., radiometersondes or meteorological satellites); by indirect estimates of each of the individual physical sources of heat (Kasten et al. [8]), and by diagnostic use of the equations of motion (Wiin-Nielsen and Brown [19]). We have chosen the second of these because unlike the third method it permits separate estimates of each of the principal heating components (condensation, radiation, and conduction) and is more closely allied with the methods used for introducing heating into multi-level numerical prediction models. Instrumentation has not yet been developed to the stage where all of the heating components may be determined.

In the conclusion of this paper some remarks will be made regarding the computation of heating fields by satellites and multi-level models. Here it will be noted that in spite of significant progress, there are still many serious obstacles to overcome before attaining the full realization of these two most promising developments.

The procedure chosen by the authors for computing atmospheric heating requires the collection and processing of many special types of local weather data most of which (such as cloud and pyrheliometric observations) cannot be easily processed by electronic computers. Therefore only a limited sample of data at a few stations and for limited time periods has been worked up so far. This greatly restricts the generality of the conclusions which can be drawn. Nevertheless, the authors feel that enough information of general importance has been gleaned from this limited sample to justify bringing it to the attention of interested persons.

Total heating is computed using the heat-balance method, which consists of estimating and summing the contributions of each of the major components: namely, long-wave radiative cooling, short-wave heating by absorption of solar and sky radiation, condensation or evaporation in clouds, and sensible heating by turbulent contact with the ground. This particular method has been utilized over the years with varying success by many researchers, but usually only for yearly or seasonal averages (Albrecht [1]) or for selected heating factors (Kasten et al. [8]). The data used for the present study consist of estimates of each of the heat sources for three layers of the troposphere (1000–600, 600–200, and 1000–200 mb.) averaged over an area of 15-mi. radius centered at Washington, D.C., and for each successive 12-hr. period from June 1 to July 31, 1961 (122 cases). The procedure embraces several fields of physical meteorology and will not be discussed in detail in this report. For a full discussion, together with tables of the different heating factors, the reader must be referred to an unpublished research report (Clapp, Winninghoff, and Fisher [3]) copies of which may be obtained on request by writing to the Extended Forecast Branch, NMC, U.S. Weather Bureau, Washington, D.C.

The most critical and yet most difficult-to-measure factors in obtaining the local heat budget by this method are the cloud amounts, types, and elevations of base and top. It was necessary to idealize the clouds by grouping them into four basic types: low clouds, divided into cumulus and stratus, middle clouds, and high clouds. A constant height of base and top was assigned to each type. Cumulus and stratus clouds were not allowed to occur together. The local radiosonde data were then averaged into 36 different groups depending on the 12 possible combinations of these 4 cloud types (including clear cases) and 3 temperature classes (cool, moderate, and warm). Cloud type and amount for each 12 hr. were estimated largely from the hourly synoptic observations.

Using the appropriate average upper-air sounding and idealized cloud structure for each 12-hr. interval, the long-wave radiative cooling for the different layers was computed using an Elsasser radiation diagram (Elsasser [5]) and the short-wave absorption by an empirical formula devised by one of the authors. The heating of the entire atmosphere caused by direct turbulent contact with the ground (sensible heating) was obtained from a heat-balance equation for the ground, in which the sensible heating is a residual between long-wave cooling and short-wave heating of the ground, evaporation, and local storage of heat in the ground. Since evaporation and short-wave absorption could be estimated only for 24-hr. intervals, no diurnal variation of sensible heating could be obtained.

Condensation and evaporation in the air were determined using an estimate of the average 12-hr. rainfall in the 15-mi. radius region, together with the cloud structure and a rough approximation to the vertical motion within the clouds. This procedure is based on the assumption that rainfall is a true measure of the net condensation and evaporation in the air over the chosen space-time domain, an assumption which is valid if there is no storage of condensed moisture and no "spill-over" of rain between adjacent domains.

The most difficult factor to measure was the vertical eddy flux-divergence of heat (vertical redistribution of heat between layers due to small-scale eddies). Only crude estimates were made of the eddy redistribution of the heat picked up from the ground and that released within precipitating cumulus clouds.

These empirical or semi-exact methods, together with the usual lack of sufficient data, make difficult a quantitative assessment of errors. However, a general "feeling" for the validity of physical estimates suggests that the computations are reasonably good for the entire troposphere and considerably less so for the two sub-layers (mainly because no adequate estimates could be made of the turbulent redistribution of heat within the atmosphere.) Because of the omission of some diurnal effects, the justification for making estimates for individual 12-hr. periods is questionable. However, the average statistics presented here are probably not greatly influenced by diurnal changes.

2. THE OVERALL SYNOPTIC SITUATION

The following information regarding the average state of the circulation and its departure from normal during June and July 1961 has been taken mainly from reports by Stark [17] and Green [6]. The reader is referred to these for mean weather and circulation charts (which will not be reproduced here) and for further details.

The observed precipitation and temperature patterns for the United States for both months were characterized by abnormally low temperatures in the south central United States with strong east-west temperature contrasts along the eastern seaboard. Both also showed a band of heavy precipitation extending from the Gulf States northeastward, attesting to vigorous frontal and cyclonic activity. This was accompanied by abnormally low heights aloft in the same areas, shown by the monthly-mean 700-mb. charts and their anomalies for the Northern Hemisphere, with the long-wave trough (lowest latitude of 700-mb. contours) being far west of its normal position. In other areas the circulation aloft was quite different for the two months. June showed a vigorous, large-amplitude wave system over much of the hemisphere whereas July was characterized by "blocking" at high latitudes, with a rather sluggish westerly (anomalous easterly) circulation just north of the latitude of Washington. Mean circulation patterns for the first and second half of each month show that the large-amplitude wave situation lasted from about mid-June to mid-July.

Washington, D.C., was situated just to the east of cool air masses flooding the central portion of the country. In June, it lay directly within the belt of heaviest rainfall, while in July it was just south of this. For the two months as a whole, Washington's precipitation averaged about half an inch and temperature half a degree above normal. The thickness between 1000 and 200 mb. averaged 117 ft. below normal, indicating (with the positive surface anomaly) a steeper than normal lapse rate.

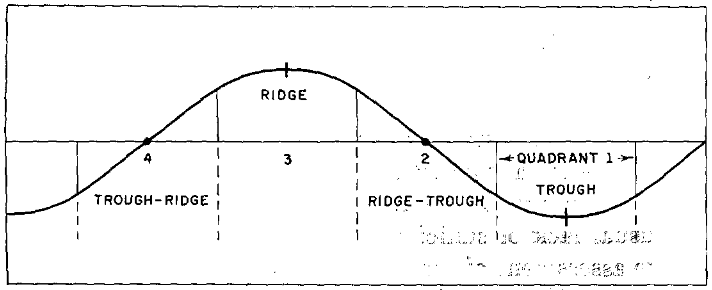

FIGURE 1.—Schematic pressure wave at 700 mb. showing definition of quadrants used in compiling table 1.

TABLE 1.—*Number of cases by amplitude-quadrant classes, and average amplitudes and wavelengths for upper waves at 700 mb. at Washington, D.C. See text and figure 1 for explanation*

Range of amplitude (ft.)	20–160	170–300	300–740	(1)
Average amplitude (ft.)	88	225	460	268
Average 1/2 wavelength (° long.)	17	28	45	31
Quadrant:				
1	11	18	31	60
2	11	7	4	22
3	12	9	3	24
4	2	9	5	16
All Quadrants	36	43	43	122

[1] All amplitudes.

From these circulation characteristics, one might conclude that heating at Washington in this period and its relation to the circulation must have been typical of a summer season cooler than normal. It is certain that the average tropospheric heating was greater than normal, since, as will be shown later, it is largely dependent on total rainfall.

3. HEATING RELATED TO THE LONG WAVES

To investigate the relation of diabatic heating to the long waves in the westerlies, the data for each 12-hr. period were first grouped according to the location of Washington in one of four quadrants of the upper waves found on each of the 0000 and 1200 GMT 700-mb. charts. The quadrants were defined in terms of the relative (or angular) distance between trough and ridge, as shown in figure 1. The ridge or trough location was determined as the longitude where the closest significant ridge or trough line intersected the latitude of Washington. A trough or ridge line is defined as the axis of minimum or maximum latitude of the 700-mb. contours. The inflection points of the wave (quadrants 2 and 4 in fig. 1) were assumed to lie halfway between trough and ridge. The amplitude of each wave was defined as the difference in 700-mb. height, and the half wavelength as the difference in longitude, between the ridge and trough at the latitude of Washington.

Next the 122 cases were separated into three approximately equal parts according to wave amplitude, and the average amplitude and wavelength determined. The results are shown in table 1 along with the number of cases in each of the 12 amplitude-quadrant classes. It is interesting to note that as the average amplitude increases, so does the half wavelength, although at a relatively slower rate. This is in accord with what is known about the relative horizontal scales of the large waves in the westerlies.

Finally, average values of each of the principal heating components were obtained for each amplitude-wavelength class and for each of the three pressure layers (1000–600 mb., 600–200 mb., and 1000–200 mb.). The results for 1000–200 mb. are summarized in the schematic wave patterns shown in figures 2, 3, and 4. Also plotted in these figures are the corresponding average thickness between 1000 and 200 mb.

These patterns constitute composite time cross-sections showing the variation of thickness and heating as the upper waves pass the vicinity of Washington. To the extent that the waves move from west to east without significant change in structure, these diagrams also may be interpreted as average space cross-sections at the latitude of Washington. This is perhaps a fair approximation for continental regions to the west of Washington, but significant changes in some of the heating parameters and in thickness must be expected to the east over the Atlantic Ocean. Thus, in summer over land the air probably is almost continually heated from below over 24-hr. intervals by direct contact with the ground, as shown by the long-dashed curve marked P_G in the diagrams. But over the ocean in summer, little heat is transmitted from sea to air (Jacobs, [7]), so that the turbulent component probably decreases sharply there. At the same time convection is suppressed, temperature is lower (and therefore thickness is less), and radiational cooling is larger than over the land. A true cross-section along a latitude circle would probably show considerably more heating over the land than over the water for any corresponding wave quadrant.

Before discussing the figures it should be pointed out that for ease in visual interpretation the smooth curves have been drawn freehand despite the fact that the average data were computed only for the four wave quadrants indicated by the vertical lines. Also, the number of cases in some of the quadrants for the low and high amplitude waves is rather small (see table 1). Therefore one cannot be certain of the exact amplitude and phase.

Figure 2 shows the distribution of the parameters relative to the troughs and ridges for waves of all amplitudes. The expected relation between the thickness and pressure waves is found, the former lagging behind the latter, in this instance with a phase difference of about 45°. The total heating (heavy solid curve) appears to be dominated by condensation heating (dashed curve) which has an amplitude (see inset) about four times that of any other heating component. (Note: The "amplitude" in this and the other figures is the difference between the largest and smallest *computed* value, and not the difference between the maximum and minimum of each curve.) There is a weak tendency for the heating components to be "in phase" with each other, as shown by the fact that the amplitude of total heating is greater than that of any one of them.

The relation between total heating and thickness (a measure of mean tropospheric temperature) is important for the maintenance of the thermal contrasts (i.e., potential energy) of the waves. It is obvious that if the air is heated when it is warm and cooled when it is cold, there will be a tendency to increase the amplitude (potential energy) of the waves, or at least to maintain it against dissipative forces (e.g., transformation from potential to kinetic energy). In this instance it is clear that total heating and thickness are positively correlated, especially in the vicinity of the thermal ridge.

This tendency for positive generation of potential energy in the waves of the time cross-sections has been expressed in more quantitative fashion through use of integral theorems for generation of available potential energy introduced by Lorenz [12]. This quantitative aspect will be taken up in the following section. Here, it will be pointed out that local maintenance of potential energy in the time cross-sections is only part of the local contribution to total and eddy available potential energy.

Figure 3 shows the distribution of parameters for all low-amplitude cases. The thickness field is more out of phase with the pressure field (i.e., shows a greater lag) than is the case for all amplitudes. This is to be expected for the smaller-scale wave systems, which perhaps may be identified with developing wave-cyclones. The most striking change is the sharp decrease in amplitude of condensation heating and with it the amplitude of total heating. (Compare insets of figs. 2 and 3.) Apparently in this instance summer rainfall had a tendency to occur almost randomly with respect to troughs and ridges, but with a slightly greater tendency to occur in the ridge area of the waves. Despite this, the different heating components still tend to be in phase, since the amplitude of total heating is almost twice as great as that of any single component. Long-wave cooling tends to be definitely out of phase with the other components. Total heating is more strongly in phase with thickness than in the case of waves of all amplitudes, indicating a more efficient production of potential energy.

Figure 4 corresponds to the cases of large-amplitude waves. The most striking change from figure 3 is that the amplitude of condensation heating has increased by a factor of 10 (compare insets of figs. 3 and 4) completely dominating the curve for total heating. The amplitudes of the other components and of thickness increase too, but only by factors of 20 percent to 50 percent. Apparently as the long waves increase in amplitude, a much more efficient organization of condensation takes place, most of the rainfall being concentrated near the inflection point between the trough and downstream ridge. These results may be compared to a similar finding by Klein [9] for precipitation in the Tennessee Valley. His schematic diagram (not reproduced) showing precipitation related to the long waves shows that for large-amplitude systems most rainfall occurs just east of the wave troughs, whereas for small amplitudes rainfall occurs in and even to the east of the ridges.

Figure 4, as compared to figure 3 also reveals interesting phase shifts. The temperature wave shifts to the right in the diagram, so as to become more in phase with the pressure waves, since the large-amplitude systems probably represent fully-developed or occluded cyclones. The phase of total heating on the other hand, shifts in just the opposite direction (to the left in the figures) so as to become more out of phase with the pressure wave, and therefore becomes almost 90° out of phase with the temperature wave. The quantitative study of local potential-energy generation discussed in the next section shows that such a relative phase shift is essential, because otherwise the increased amplitude of both thickness and total heating would lead to an altogether too large production of potential energy. Even with the phase shift the production of energy for the large-amplitude waves is much greater than that for the small ones.

The patterns of heating and thickness relative to the pressure wave for the lower half of the troposhere (1000–600 mb., not shown here) are quite similar to those for the entire troposphere, except in the case of long-wave radiational cooling which becomes of significantly larger amplitude and in phase with total heating. This result is due to the fact that during times of abundant rainfall, cloud masses extend up through the 500-mb. level. The clouds greatly reduce, or may even cancel altogether, radiational cooling below the 500-mb. level, whereas at times of clearing and little precipitation the radiational cooling increases. Thus there will tend to be a positive correlation between the net heating effect of long-wave radiation and precipitation (and therefore total heating) in the lower troposphere. On the other hand, increased moisture near cloud tops leads to much larger radiational losses in the upper part of the troposphere, and therefore to a negative correlation there between radiational heating and precipitation. Thus there is compensation in the two halves of the troposphere resulting in the slightly negative correlation between long-wave radiational heating and total heating, shown in figures 2 to 4.

It occurred to the authors that since total heating is dominated by condensation (see figs. 2 and 4), and since local condensation in the Washington area in summer is very erratic, the results shown in figures 2, 3, and 4 might not be typical of synoptic-scale systems; i.e., if condensation heating had been computed over a larger region, more characteristic of the scale of weather maps, the results might be quite different.

In an attempt to throw light on this matter, average 12-hr. rainfall (proportional to condensation heating in the 1000–200-mb. layer) was also determined in a much

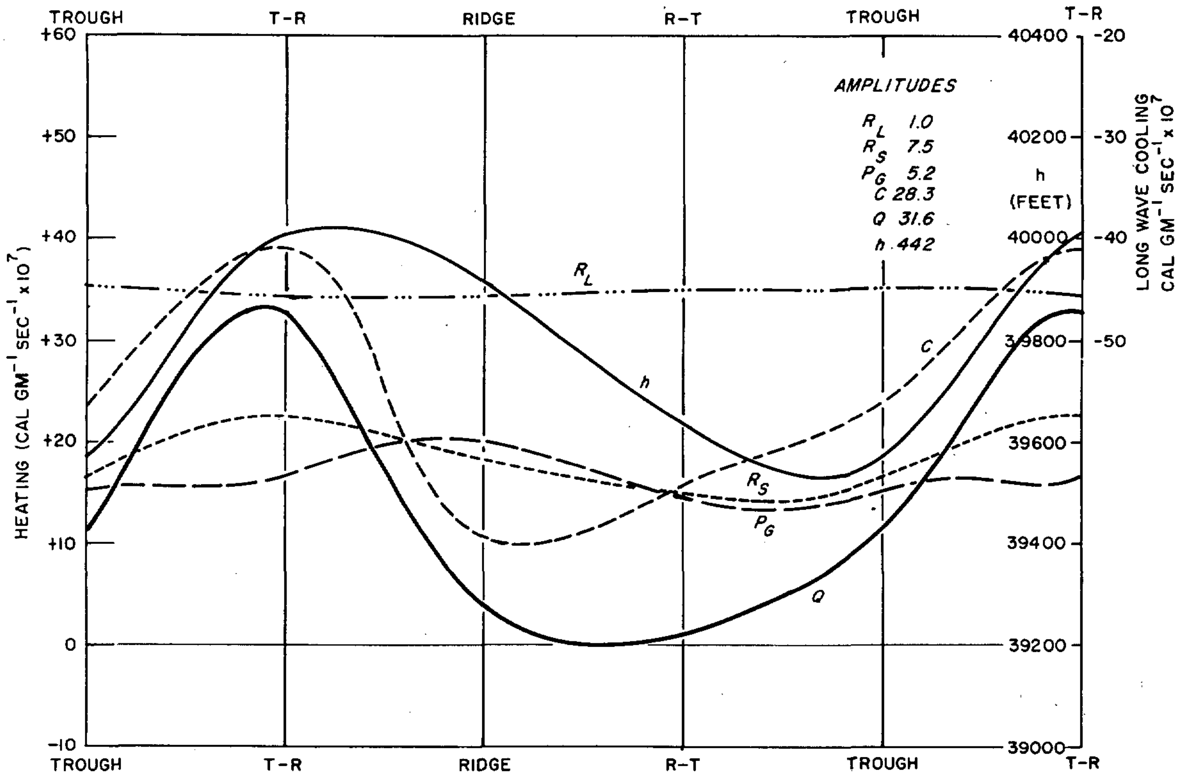

FIGURE 2.—Distribution of tropospheric heating and thickness in layer 1000 to 200 mb. relative to upper waves of all amplitudes at 700 mb. Compiled for 122 12-hr. periods at Washington, D.C., June and July 1961. Symbols are: h, thickness; R_L, long-wave cooling; R_s, absorption of short-wave radiation; P_G, heating by turbulent contact with ground; C, heating by condensation and evaporation; and Q, total heating (sum of all components). Scale of thickness and long-wave cooling at upper right. Scale of all other heating components at left. Inset: Amplitude of heating components. See scale for units.

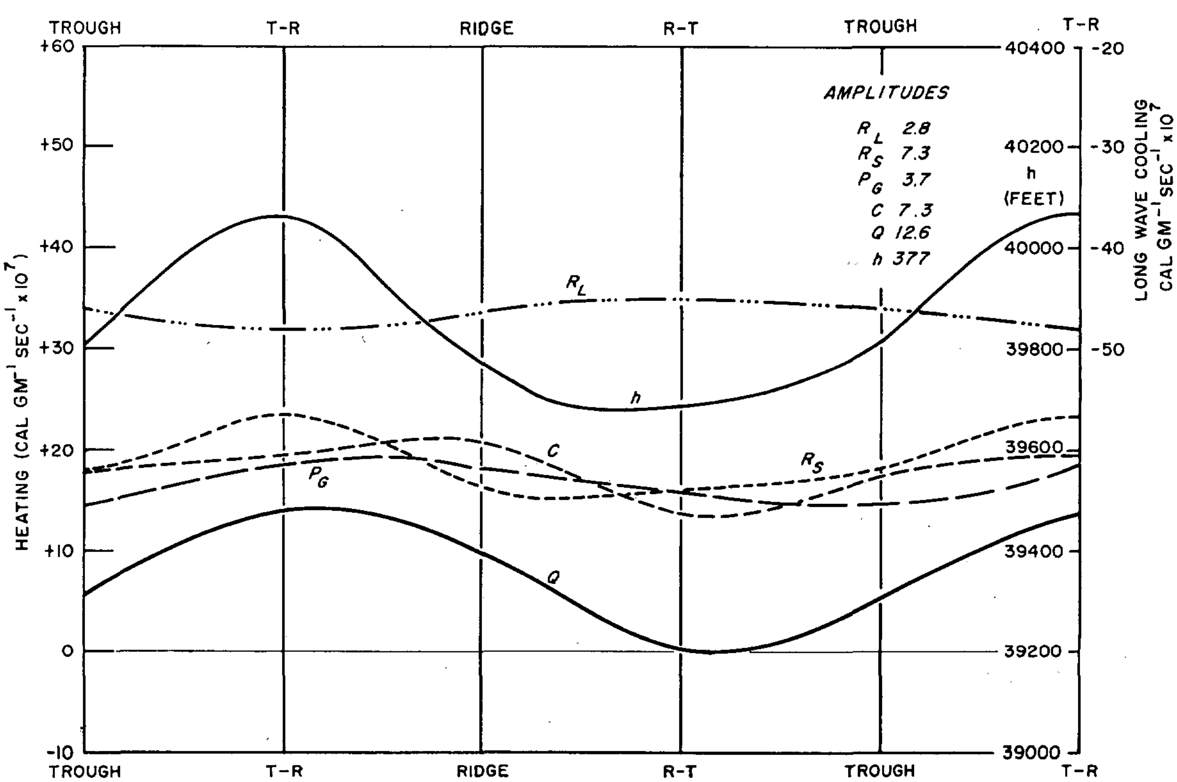

FIGURE 3.—Heating and thickness relative to waves of small amplitude, for 36 12-hr. periods. See figure 2 and text for explanation.

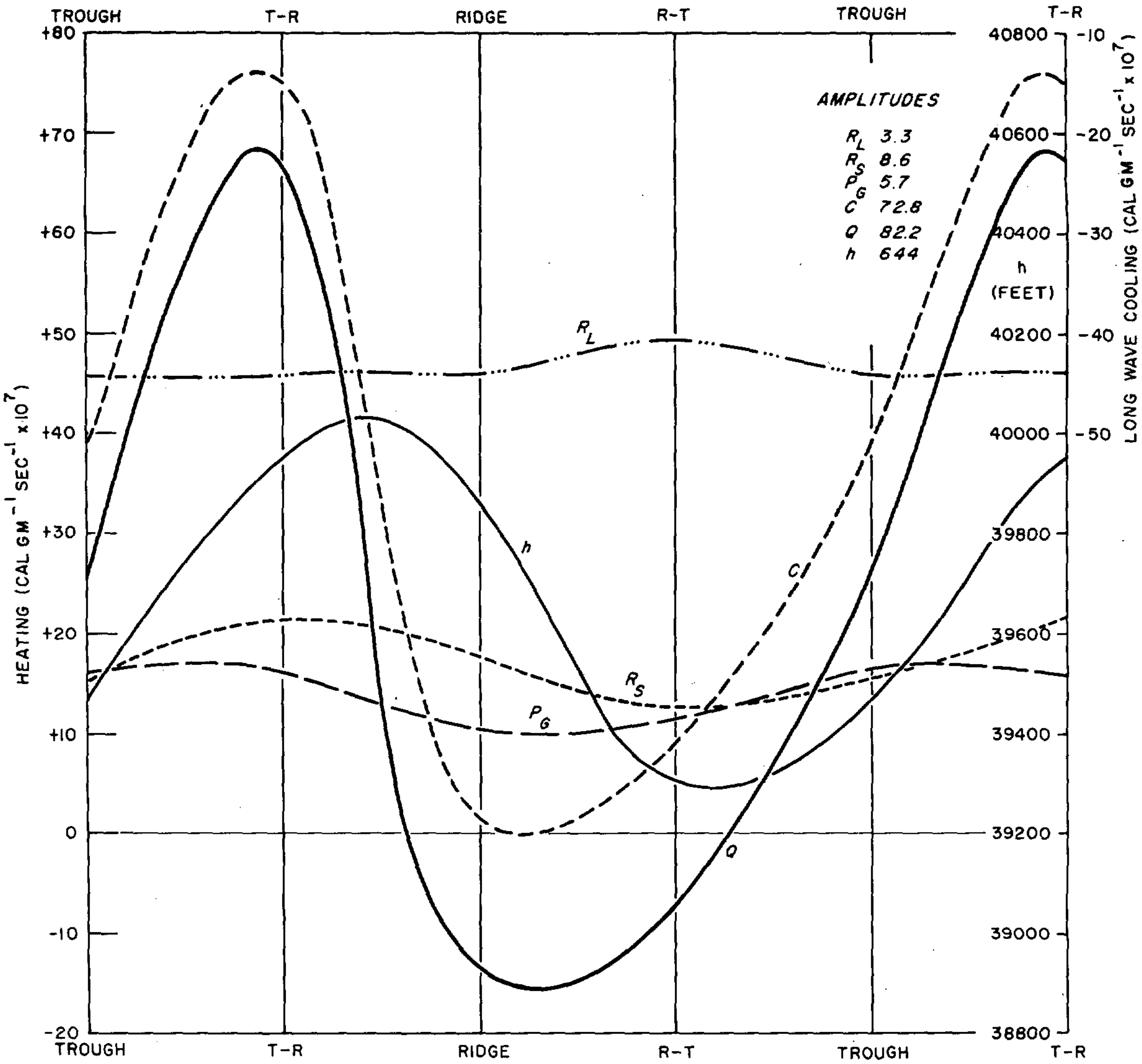

FIGURE 4.—Heating and thickness relative to waves of large amplitude, for 43 12-hr. periods. See figure 2 and text for explanation.

larger (40-mi. radius) area surrounding Washington. Condensation-heating curves similar to those in figures 2 to 4 were constructed. These showed no significant phase change, but an increase in amplitude in each case which was important only in the case of the small-amplitude wave systems. Therefore, qualitatively the results are the same; i.e., a significant positive generation of potential energy at all scales of waves is still present. However, it does not follow from this that these results are typical of all summer seasons at Washington. The large variability of rainfall for similar synoptic situations might give quite different results for other years.

4. THE GENERATION OF AVAILABLE POTENTIAL ENERGY

An expression for the local contribution to the generation of total global available potential energy may be derived from the definition of this quantity as stated in equation (4.4) of Wiin-Neilsen and Brown [19]. If we include integration through time as well as space, their equation may be expressed in our notation as follows:

$$g_A = -\frac{R}{\gamma c_p t S}\int_S \int_0^{p_0} \int_0^t \frac{1}{p}\frac{\partial z}{\partial p} Q dt dp dS \qquad (1)$$

Here, R is the gas constant for dry air, γ, a mean static stability; c_p, specific heat of dry air at constant pressure; p, pressure at any level; p_0, pressure at the ground; z, height of an isobaric surface; Q, individual rate of heat addition per unit mass; t, a time interval of the order of a month or season; and S, area of the earth's surface. It can be seen that g_A is a measure of the average generation of global available potential energy per unit area and time, and may be expressed, for example, in ergs cm.$^{-2}$ sec.$^{-1}$

The integrand of this equation states that there will be a positive contribution to the total generation of available potential energy in those localities where the air is being heated when it is warm and cooled when it is cold. (Note that $\partial z/\partial p$ is related to temperature through the hydrostatic equation and equation of state.) The physical significance is that when these individual local contributions are summed through time and through the entire volume of the atmosphere, the net contribution g_A must be balanced by an increase in zonal or meridional temperature contrasts (i.e., by an increase in total available potential energy) and/or by a transformation from potential to kinetic energy. This is expressed mathematically in Wiin-Nielsen and Brown's equation (4.3) which will not be discussed further here.

If we designate a time mean by an overscore, then the local contribution to the total generation for a thin vertical layer of pressure-thickness Δp may be defined as follows:

$$g_{AL}=\frac{R}{\gamma c_p P}\overline{hQ} \tag{2}$$

where h is the thickness and P is the average pressure of the thin layer.

It is next convenient to express both thickness and heating by their time mean value plus a departure from that mean, the latter being designated by a "prime" superscript. The local contribution term then becomes:

$$g_{AL}=\frac{R}{\gamma c_p P}(\bar{h}\overline{Q}+\overline{h'Q'}) \tag{3}$$

The first term inside the parentheses of equation (3) tends to be very large, usually one order of magnitude larger than the second term. This means that it will be very sensitive to small errors in the time-averaged quantities, and these errors will obscure the second term, which can be determined with reasonable precision. To partly overcome this inconvenience, we can take advantage of the fact that the largest part of the first term integrates out to zero. This is due to the fact, pointed out by Wiin-Neilsen and Brown, that the value of heating averaged through space (in a constant pressure surface) and time must be close to zero.

To take advantage of this, it can be shown that it is only necessary to replace $\bar{h}$ by its departure from its global average for the same period of time. This departure will be designated by a double-prime superscript. If in addition the second term in equation (3) is modified by using the definition of the simple linear correlation coefficient relating local time variations in thickness and heating, the local generation term becomes:

$$g_{AL}=\frac{R}{\gamma c_p P}(\bar{h}''\overline{Q}+r_{h,Q}\sigma_h\sigma_Q) \tag{4}$$

where $r_{h,Q}$ is the correlation coefficient, and σ_h and σ_Q are respectively the local standard deviations of thickness and heating.

An expression for the local contribution to the generation of eddy-available potential energy (designated by g_{EL}) may be derived in a similar fashion. This is an expression of the effect of heating in maintaining west-east thermal contrasts along latitude circles, and therefore is one of the important factors in the maintenance of the long waves in the westerlies. The expression will not be derived here. If time variations in the zonal (latitudinal) averages of h and Q may be neglected, one finds:

TABLE 2.—*Components of the local contribution to available potential energy at Washington, D.C. Summer 1961. Amplitude of waves listed in table 1. Pressure layers are in mb.; N, number of cases; σ_h, standard deviation of layer thickness in ft.; σ_Q, standard deviation of heating in cal. gm.$^{-1}$ sec.$^{-1}\times 10^7$; r, time correlation between h and Q; $(g_{AL})_2$ correlation term of local generation in erg cm.$^{-2}$ sec.$^{-1}$*

Amplitude	Layers	N	σ_h	σ_Q	$r\times 100$	$(g_{AL})_2$
All	1000–200	122	406	58	20	970
	1000–600		149	52	22	1070
	600–200		272	68	15	
Low	1000–200	36	310	47	29	859
	1000–600		111	44	44	815
	600–200		216	53	14	
Medium	1000–200	43	435	37	28	900
	1000–600		150	35	32	983
	600–200		296	43	19	
High	1000–200	43	389	78	32	1947
	1000–600		153	67	25	2510
	600–200		257	90	30	

$$g_{EL}=\frac{R}{\gamma c_p P}(\bar{h}^*\overline{Q}^*+r_{h,Q}\sigma_h\sigma_Q) \tag{5}$$

where the asterisk indicates departure of a quantity from its zonal average. The first term of equation (5) is seen to be the local contribution to eddy generation by the so-called "standing eddies" (semipermanent waves in the westerlies) while the second term is identical to that in equation (4).

The second term of equation (4) or (5) was evaluated using the Washington data for the 2-month period, obtaining separate values for the entire troposphere (considered as one pressure layer) and for the sum of the two sub-layers. The 122 cases were further subdivided into the three amplitude groups defined in section 3, table 1. The results are summarized in table 2. The last column of this table, labeled $(g_{AL})_2$ is the second term (correlation term) of equations (4) and (5) multiplied by the constant coefficient which was evaluated using $R=2.87\times 10^6$ erg gm.$^{-1}$ °K.$^{-1}$; $c_p=0.24$ cal. gm.$^{-1}$ °K.$^{-1}$; $\gamma=3\times 10^{-4}$ cm.^{4} gm.$^{-2}$ sec.^{2} (Wiin-Nielsen and Brown [19]); and with the mean pressure of the layer (P) being 600, 800, and 400 mb. for the layers 1000–200, 1000–600, and 600–200 mb., respectively. The energy-production for both layers (last number in second row of each amplitude group) was evaluated by computing $(g_{AL})_2$ for each layer separately and then summing the two.

Some of the more interesting results shown in this table may be summarized as follows:

1. The sum of the energy production for the two layers is greater than that for the single layer (1000–200 mb.). This suggests that even larger values might be obtained if heating were known as a function of pressure.

2. The magnitude of the energy production increases steadily with wave amplitude and is three to four times

TABLE 3.—*Components of the local contribution to total available potential energy at Washington, D.C., summer 1961. All values for entire troposphere (1000–200 mb.) and for all 122 cases. h is thickness of the layer in ft.; overscore, 2-month average; bracketed value, estimate of global average; double-prime superscript, difference between columns 1 and 2; Q, local heating in cal. gm.$^{-1}$ sec.$^{-1}$ $\times$ 10^7; $(g_{AL})_1$, first term of equation (4)*

$\bar{h}$	$\{\bar{h}\}$	$\bar{h}''$	$\bar{Q}$	$(g_{AL})_1$
39,710	39,334	+376	11	836

as large for the large-amplitude waves as for the small ones.

3. The correlation coefficient between heating and thickness averages +0.20. This means that significant amounts of energy are produced despite the fact that temperature and heating are almost 90° out of phase. This suggests that at least the correct phase of the heating wave must be established if meaningful values of potential energy production are to be obtained by this or any other procedure (e.g., in numerical prediction models).

The first term of equation (5) *cannot* be evaluated at all using the data of this project. However, a crude estimate can be made of the first term of equation (4) if we may assume that the global average thickness for the two months (defined here as $\{\bar{h}\}$) is given approximately by its equivalent normal value. The latter in turn may be approximated by the average thickness for both summer and winter over the Northern Hemisphere, using normal height data from London [11]. Because of the questionable accuracy of this term, it was computed only for the entire troposphere and all 122 cases. The elements of this computation are summarized in table 3.

It can be seen that the first term of equation (4) is positive and about the same magnitude as the second term (first row, last column of table 2). The sum of the two is 1806 erg cm.$^{-2}$sec.$^{-1}$, a value close to the various estimates of the frictional dissipation of kinetic energy. In the long run the global production of available potential energy, the conversion from potential to kinetic energy, and the frictional dissipation of kinetic energy must be approximately equal. Therefore the above result suggests that during these two months heating in the Washington area produced its fair share of potential energy.

5. HEATING RELATED TO THERMAL ADVECTION

In the hydrodynamic equations for multi-level numerical prediction models, diabatic heating is introduced through the thermodynamic energy equation, which may be written as follows:

$$Q=c_p\left(\frac{\partial T}{\partial t}+\mathbf{V}\cdot\nabla T\right)+c_pT\omega\,\frac{\partial \ln \theta}{\partial p} \qquad (6)$$

Here Q is the individual rate of heating and cooling per unit mass; c_p, specific heat at constant pressure; T, absolute temperature; $\mathbf{V}$, horizontal wind component; ∇, horizontal gradient vector; ω, vertical pressure-velocity; and p and t pressure and time, respectively.

Heating computed by the heat-balance method was compared to each term and to the sum of the terms on the right side of equation (6). For this purpose the terms were estimated at Washington for each of the 122 0000 and 1200 GMT synoptic times during June and July 1961, and for each of 6 levels (sea level, 850, 700, 500, 300, and 200 mb.). Data were read from routinely analyzed charts of the Weather Bureau's Analysis and Forecast Branch. Standard finite-difference methods were used, with a 24-hr. centered time step, a horizontal grid interval (i.e., twice the distance from Washington to each of four surrounding grid points) of 5° latitude aloft and 2.5° at the ground, and a varying vertical interval equal to the pressure difference between adjacent levels below and above the level in question, except at the ground where a noncentered pressure difference was used. Observed winds at Washington were used in estimating horizontal temperature advection. Horizontal divergence at each level was computed by the kinematic method from winds estimated at the four grid points from analyzed streamlines and isotachs. From these values of divergence, the vertical gradient of ω was estimated from the continuity equation, and ω itself computed at each level by a summation procedure, starting with a value of zero at the ground.

Estimates of divergence and vertical motion for individual synoptic charts are subject to large random errors. In the particular method used here, the horizontal wind at the grid point to the east of Washington was especially difficult to estimate since the point lies in a sparse data region over the ocean. Perhaps for this reason, a strong bias toward too much convergence was obtained. To minimize this, the vertical motion was recomputed assuming the mean divergence to be zero in the layer 1000–200 mb. (As will be noted later, this may be too drastic a suppression of divergence.) To further minimize random errors in this term, as well as in the other terms and in the computations of heating by the heat-balance method, each of these was averaged for the layers 1000–600, 600–200, and 1000–200 mb. and for each of 25 partly overlapping 5-day periods during the two months.

Before taking up the results, it might be profitable to anticipate what might be expected from a knowledge of the physical processes themselves. From the discussion in section 3 it is apparent that for these two months the total heating was dominated by condensation whenever this occurred. Condensation in turn is directly proportional to the upward motion found in precipitating clouds. Also, it may be anticipated that on many clear days when net cooling occurs, downward motion will be found with subsiding anticyclonic weather. Therefore a *positive* correlation between heating and the vertical advection term is to be expected. It can also be expected that the vertical advection term tends to have the opposite sign to that of the sum of the other two terms, especially when averaged through deep layers of the atmosphere. If this were not true, vertical motions which have frequently been com-

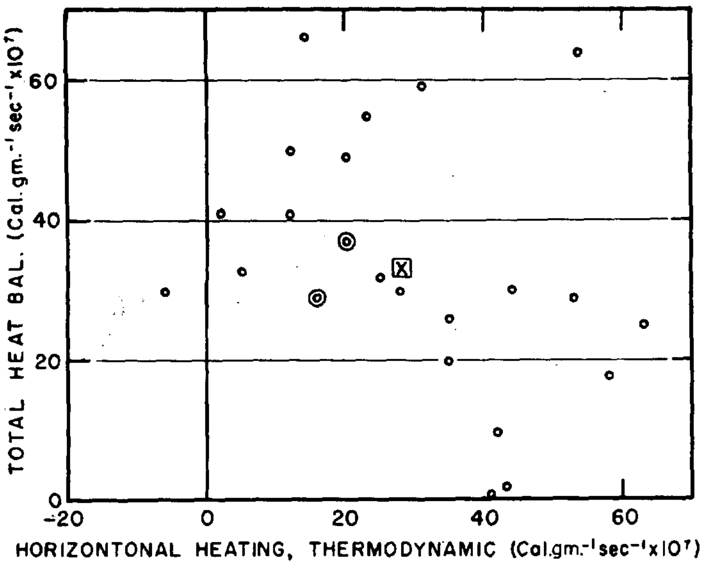

FIGURE 5.—Sum of first two terms of thermodynamic energy equation (equation (6), "horizontal heating") vs. total heating by heat-balance method, both averaged for layer 1000 to 600 mb. and for 25 partly overlapping 5-day periods at Washington, D.C., June and July 1961. Average of both quantities shown by square with cross. Circled dots indicate two cases. Correlation coefficient is −0.34.

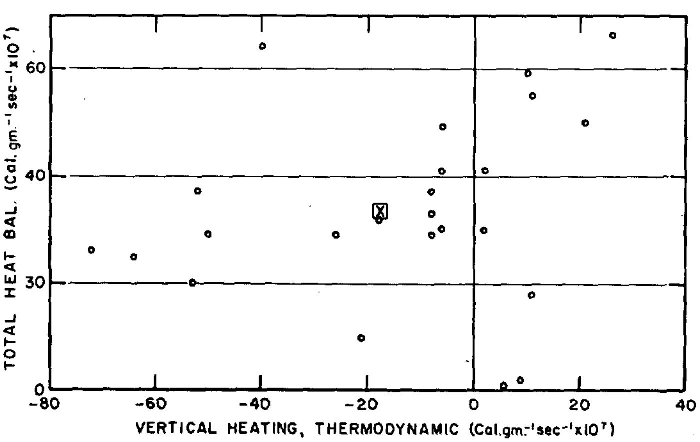

FIGURE 6.—Last term of thermodynamic energy equation (equation (6), "vertical heating") vs. total heating by heat-balance method. See figure 5 for explanation. Correlation coefficient is +0.20.

puted by the adiabatic method (equation (6) with Q zero) would be valueless. For this reason, a *negative* correlation between heating and the sum of the first two terms (called hereafter the horizontal term) may be expected.

The results for the layer 1000–600 mb. are shown in figures 5 and 6. As anticipated, there is a positive (negative) correlation between heating and the vertical (horizontal) term, but the magnitudes of the coefficients are surprisingly low, especially for the vertical term. These low correlations are associated with an equally low (but slightly positive) correlation between total heating as computed by the heat balance and thermodynamic

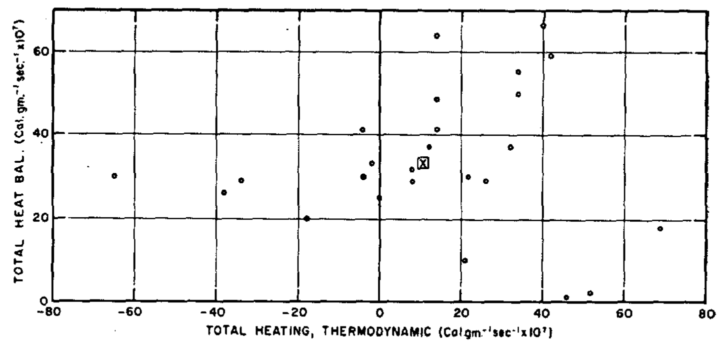

FIGURE 7.—Total heating by thermodynamic energy equation method vs. total heating by heat-balance method. See figure 5 for explanation. Correlation coefficient is +0.01.

methods (fig. 7) despite the fact that these two estimates ought to be equal in accordance with equation (6). Aside from random errors in the calculations, which are especially troublesome for the vertical term, the cause of this poor relationship may be traced to the different space scales of the two estimates. The heat-balance calculations apply to a 15-mi. radius area (700 mi.^{2}) while the finite-difference thermodynamic method represents average heating for a 120,000-mi.^{2} region. Because of the sporadic nature of summer shower type precipitation, it is likely that at least the contribution of condensation to total heating may be quite different over the two regions.

In an attempt to eliminate this probability of non-representativeness in the two estimates, four clear-cool days and four days of widespread precipitation were selected, each set therefore consisting of eight individual 12-hr. periods. The rainy days were selected so that there could be little doubt that the Washington-area rainfall was representative of that in the larger synoptic region. (For example, rainfall over the 40-mi. radius area was only slightly larger than that in the 15-mi. radius region on those days.) Heating by each of the two methods was then averaged for each 4-day set and for the three layers. The results are shown in table 4. This composite technique reveals quite satisfactory qualitative agreement between the two methods. Both show net cooling of the entire troposphere on the clear-cool days, with the greatest cooling in the upper troposphere, and net heating on the rainy days with the largest heating in the lower troposphere. Furthermore, the signs of the horizontal and vertical heating terms are as anticipated. Unfortunately, the quantitative comparison is still not very good. The thermodynamic method appears to introduce consistently more cooling (less heating) than the heat-balance method. This analysis does not reveal which may be nearer correct, but it can be said with some certainty that the thermodynamic method gives too much cooling in the clear cases. Even if short-wave absorption and turbulent heating were zero (the only important sources of heat in the clear cases) a maximum cooling by long-wave radiation alone of −43 units (−304 ly./day) could be expected in the layer

TABLE 4.—*Average heating in three selected pressure layers for four clear-cool and four general-precipitation days computed by the heat-balance and thermodynamic energy-equation methods. Values for the horizontal and vertical heating terms for the total layer are also given for the themodynamic method. Units: cal. gm.$^{-1}$ sec.$^{-1}\times 10^7$*

Pressure interval (mb.)	Clear and cool				General precipitation			
	Heat balance method	Thermodynamic method			Heat balance method	Thermodynamic method		
		Ave.	Horiz.	Vert.		Ave.	Horiz.	Vert.
1000–600	7.4	−13.5			134.5	69.1		
600–200	−33.1	−72.1			122.0	66.1		
1000–200	−12.5	−43.0	+83.4	−126.4	128.3	67.6	−21.0	+88.6

1000–200 mb. Perhaps one reason for this discrepancy is the introduction of the "zero-divergence" assumption in computing vertical motion, which may have gone too far in correcting for over-convergence.

6. SUMMARY AND CONCLUSIONS

Computations of heating and cooling in deep layers of the troposphere, produced by short- and long-wave radiation, condensation, and turbulent exchange with the earth's surface, were used to obtain some relationships with circulation and weather near Washington, D.C., for June and July 1961. Perhaps the greatest value of such estimates of local heating lies in their potential use for computing geographical patterns of the local contribution to the generation of available potential energy averaged over long periods of time (months or seasons). This might throw light on the influence of local energy-source anomalies on the maintenance of the general circulation. One possible computational procedure has been discussed in section 4.

The computation of heating used here, even though now being revised for fast processing on electronic computers, is relatively slow and laborious because of the necessity of collecting special forms of local data. Therefore an attempt was made to show how the currently available satellite data may be interpreted in terms of atmospheric heat sources and sinks. This part of the study has been published earlier (Clapp [2]). Among the results is the finding that the total outgoing long-wave radiation at 200 mb. (probably proportional to the long-wave radiation measured by a satellite) has a fairly high correlation (+0.54) with the long-wave radiative cooling of the entire troposphere. Unfortunately it is less well correlated (+0.43) with the total heating from all sources. When improved instrumentation or procedures for meteorological satellites are developed to the point where better estimates of total heating are possible, one will be able to obtain in a relatively short time invaluable information on the role of heating in the maintenance or destruction of potential energy in various parts of the world.

An attempt along these lines has been made by Suomi and Shen [18] using the outgoing long-wave radiation as measured by the satellite Explorer VII. They find (using radiometersonde observations) a much higher correlation (+0.88) than we did between outgoing radiation and net long-wave radiative cooling. Assuming the satellite-measured radiation is equivalent to the net cooling, they show that there is on the average a positive generation of eddy-available potential energy over a large area of the earth. On the other hand, our results (presented in figs. 2 to 4) suggest that long-wave radiative cooling is poorly or even negatively correlated with temperature, and therefore leads to a slight destruction of potential energy. However, it should be noted that Suomi and Shen's results apply to large areas and to the cold season, while ours apply to local conditions in summer.

This study revealed significant empirical relations between tropospheric heating and certain parameters carried by even the simplest of present-day dynamical circulation-prediction models. One of the more interesting of these relationships is a significant negative correlation between heating and temperature advection in deep atmospheric layers.

More sophisticated multi-level numerical models are now being designed to include the effects of diabatic heating by estimating the various individual processes as in this study, except that condensation and evaporation are computed by a continuity equation for water vapor instead of indirectly from observed rainfall (Smagorinsky and Manabe [16]). In the design of such models, the computation of vertical motion, and therefore the accurate determination of condensation, presents special problems which are receiving considerable attention (Smagorinsky [15]). Because of the importance of condensation heating (emphasized in the present report) some special aspects of this subject will be reviewed here.

Several investigations indicate that the continuity equation for water vapor yields estimates of condensation which are far too low (e.g., Manabe [13], Kurihara [10]). At least one important factor leading to such underestimates is the use of finite-difference procedures in which only the mean divergence and therefore the mean vertical motion may be obtained over the very large minimum area which can be resolved in the usual finite-difference mesh. Actually, condensation is proportional to the mean vertical motion *within the precipitating clouds*. When most of the rainfall comes from isolated convective cloud towers, as in much of the precipitation discussed in this report, the mean vertical motion within the clouds may be very large, *even though that over the entire grid area is close to zero*. Even in the case of extratropical and tropical cyclones, a large percentage of the rainfall comes directly from convective elements which penetrate the general cloud cover, so that here too finite-difference methods will give values too small for condensation heating.

Two important errors which may be introduced by this underestimation are a sharp reduction in the magnitude and a shift in the phase of total heating relative to the thermal wave. Figures 2, 3, and 4 show that in the cases studied here only a reduction in magnitude would be involved. Perhaps this may be characteristic of summertime situations, when condensation heating dominates the other components. In this case the reduced magnitude of heating would lead to a tendency by the models to underestimate the generation of potential energy of the waves, so that they would be predicted to dissipate too rapidly by friction and other energy-destroying mechanisms.

An underestimation of condensation heating may cause a much more serious error in winter, when heating of the air by turbulent contact with the earth's surface is often very large, especially in cold Arctic air masses flowing southward off the coasts of continents (Winston [20]). This type of heating may be equal to or even larger than the concurrent condensation heating. Even more significant, it will tend to be displaced in phase toward the colder air (i.e., toward the minimum in the thickness wave shown in fig. 2) while condensation in winter still occurs far to the east of the thickness minimum.

Since turbulent heating from the ground or ocean surface tends to be rather uniform over broad areas, it can be estimated by finite-difference methods without introducing systematic error. Therefore, the net result of underestimating the magnitude of condensation in winter is likely to be an erroneous shift in phase of the total heating wave so that it is out of phase with the temperature wave (i.e., the atmosphere will be incorrectly indicated as being heated where it is cold, and vice versa). *This in turn will favor a rapid destruction of the predicted potential energy of the cyclone waves.*

ACKNOWLEDGMENTS

The authors wish to thank Miss Myrtle M. Wagner for assisting in the statistical calculations and Mr. William D. Lockhart, Mrs. Marion E. Hess, and Mrs. Sonja L. Brown for their assistance with the manuscript.

REFERENCES

1. F. Albrecht, "Untersuchungen über den Wärmehaushalt der Erdatmosphäre und seine Thermodynamische Bedeutung," *Berichte des Deutschen Wetterdienstes in der U.S. Zone*, vol. 3, No. 17, 1950, 70 pp.
2. P. F. Clapp, "Comments on 'Analysis of Satellite Infrared Radiation Measurements on a Synoptic Scale' and 'Synoptic Use of Radiation Measurements from Satellite Tiros II'," *Monthly Weather Review*, vol. 90, No. 7, July 1962, pp. 287–288.
3. P. F. Clapp, F. J. Winninghoff, and G. E. Fisher, "Vertical Distribution of Atmospheric Heating and Cooling at Washington, D.C., June and July 1961," Technical Memorandum No. 21, Numerical Weather Prediction Group, National Meteorological Center, U.S. Weather Bureau, June 1962, 71 pp.
4. R. R. Dickson, "A Synoptic Characterization of the Thermal Nature of the Earth's Surface," presented at 202d National Meeting of the American Meteorological Society, Washington, D.C. (Abstract in *Bulletin of the American Meteorological Society*, vol. 43, No. 3, Mar. 1962, pp. 92–93.)
5. W. M. Elsasser, "Heat Transfer by Infrared Radiation in the Atmosphere," *Harvard Meteorological Studies* No. 6, Harvard University, Blue Hill Meteorological Observatory, Milton, Mass., 1942, 107 pp.
6. R. A. Green, "The Weather and Circulation of July 1961," *Monthly Weather Review*, vol. 89, No. 10, Oct. 1961, pp. 414–418.
7. W. C. Jacobs, "The Energy Exchange between Sea and Atmosphere and Some of its Consequences," *Bulletin of the Scripps Institute of Oceanography*, vol. 6, No. 2, 1951, pp. 27–122.
8. F. Kasten, G. Korb, G. Manier, and F. Möller, "On the Heat Balance of the Troposphere," *Final Report*, AF61(052)–18, Johannes Gutenberg Universität, Meteorologisch-Geophysikalisches Institut, Mainz, 1959, 89 pp.
9. W. H. Klein, "Winter Precipitation as Related to the 700-mb. Circulation," *Bulletin of the American Meteorological Society*, vol. 29, No. 9, Part 1, Nov. 1948, pp. 439–453.
10. Y. Kurihara, "Considerations on the Heat and Water-Vapour Budgets over U.S.A. in January 1957," *Journal of the Meteorological Society of Japan*, Ser. 2, vol. 37, No. 6, Dec. 1959, pp. 258–273.
11. J. London, "A Study of the Atmospheric Heat Balance," *Final Report*, AF19(122)–165, Department of Oceanography and Meteorology, New York University, July 1957, 99 pp.
12. E. N. Lorenz, "Available Potential Energy and the Maintenance of the General Circulation," *Tellus*, vol. 7, No. 2, May 1955, pp. 157–167.
13. S. Manabe, "On the Contribution of Heat Released by Condensation to the Change in Pressure Pattern," *Journal of the Meteorological Society of Japan*, Ser. 2, vol. 34, No. 6, Dec. 1956, pp. 308–320.
14. J. Namias, "Influences of Abnormal Surface Heat Sources and Sinks on Atmospheric Behavior," in *Proceedings of the International Symposium on Numerical Weather Prediction in Tokyo, Nov. 7–13, 1960*, Meteorological Society of Japan, Tokyo, 1962, pp. 615–627.
15. J. Smagorinsky, "On the Dynamical Prediction of Large-Scale Condensation by Numerical Methods," *Physics of Precipitation, Geophysical Monograph No. 5*, American Geophysical Union, 1960, pp. 71–78.
16. J. Smagorinsky and S. Manabe, "A Numerical Model for the Study of the General Circulation," presented at 211th National Meeting of the American Meteorological Society, New York, N.Y. (Abstract in *Bulletin of the American Meteorological Society*, vol. 43, No. 12, Dec. 1962, pp. 673–674.)
17. L. P. Stark, "The Weather and Circulation of June 1961—A Hot, Dry Month in the West," *Monthly Weather Review*, vol. 89, No. 9, Sept. 1961, pp. 368–373.
18. V. E. Suomi and W. E. Shen, "Horizontal Variation of Infrared Cooling and the Generation of Eddy Available Potential Energy," *Journal of the Atmospheric Sciences*, vol. 20, No. 1, Jan. 1963, pp. 62–65.
19. A. Wiin-Nielsen and J. A. Brown, Jr., "On Diagnostic Computations of Atmospheric Heat Sources and Sinks and the Generation of Available Potential Energy," in *Proceedings of the International Symposium on Numerical Weather Prediction in Tokyo, Nov. 7–13, 1960*, Meteorological Society of Japan, Tokyo, 1962, pp. 593–613.
20. J. S. Winston, "Physical Aspects of Rapid Cyclogenesis in the Gulf of Alaska," *Tellus*, vol. 7, No. 4, Nov. 1955, pp. 481–499.